Image Processing for Dynamic Contrast Enhanced Magnetic Resonance Image Sequences

Stephen Keeling
Institute for Mathematics and Scientific Computing
Karl Franzens University of Graz, Austria

Image and Pattern Analysis Group, Department of Mathematics and Computer Science, University of Heidelberg

May 3, 2011

Image Processing for DCE-MRI Sequences

Summary

- Introduction to the Procedure
- Determining Tissue Transport Properties
- Reconstructing Images from Undersampled Data
- Eliminating Physiological Motion in order to Track Points:
  Registration and Segmentation

Tissue Properties from DCE-MRI Sequences

Dynamic Contrast Enhanced Magnetic Resonance Imaging (DCE-MRI): Varying the constrast helps to reveal possible pathology. [Video1] [Video2]

Tissue Properties from DCE-MRI Sequences

Dynamic Contrast Enhanced Magnetic Resonance Imaging (DCE-MRI): Varying the constrast helps to reveal possible pathology. [Video1] [Video2]

Goal: Estimate tissue transport properties to identify and to visualize pathology quantitatively:

Tissue Properties from DCE-MRI Sequences

Dynamic Contrast Enhanced Magnetic Resonance Imaging (DCE-MRI): Varying the constrast helps to reveal possible pathology. [Video1] [Video2]

Goal: Estimate tissue transport properties to identify and to visualize pathology quantitatively:

$$\begin{cases} \partial_t C + \nabla \cdot (F\boldsymbol{v}) & = & \nabla \cdot (\mathcal{D}(\boldsymbol{v})\nabla C)\,, & \Omega \times (0, T] \\ \boldsymbol{n} \cdot (\mathcal{D}(\boldsymbol{v})\nabla C) & = & 0, & \Sigma \times (0, T] \\ C & = & C_{\mathrm{AIF}}, & \Gamma \times (0, T] \\ C & = & C_0, & \Omega \times \{t = 0\} \end{cases}$$

Tissue Properties from DCE-MRI Sequences

Dynamic Contrast Enhanced Magnetic Resonance Imaging (DCE-MRI): Varying the constrast helps to reveal possible pathology. [Video1] [Video2]

Goal: Estimate tissue transport properties to identify and to visualize pathology quantitatively:

$$\left\{ \begin{array}{rcll} \partial_t C + \nabla \cdot (F \boldsymbol{v}) & = & \nabla \cdot (\mathcal{D}(\boldsymbol{v}) \nabla C)\,, & \Omega \times (0, T] \\ \boldsymbol{n} \cdot (\mathcal{D}(\boldsymbol{v}) \nabla C) & = & 0, & \Sigma \times (0, T] \\ C & = & C_{\mathrm{AIF}}, & \Gamma \times (0, T] \\ C & = & C_0, & \Omega \times \{t = 0\} \end{array} \right.$$

F = mean velocity (perfusion)

Tissue Properties from DCE-MRI Sequences

Dynamic Contrast Enhanced Magnetic Resonance Imaging (DCE-MRI): Varying the constrast helps to reveal possible pathology. [Video1] [Video2]

Goal: Estimate tissue transport properties to identify and to visualize pathology quantitatively:

$$\begin{cases} \partial_t C + \nabla \cdot (F\boldsymbol{v}) &= \nabla \cdot (\mathcal{D}(\boldsymbol{v})\nabla C)\,, & \Omega \times (0,T] \\ \boldsymbol{n} \cdot (\mathcal{D}(\boldsymbol{v})\nabla C) &= 0, & \Sigma \times (0,T] \\ C &= C_{\mathrm{AIF}}, & \Gamma \times (0,T] \\ C &= C_0, & \Omega \times \{t=0\} \end{cases}$$

F = mean velocity (perfusion)

$\boldsymbol{v}$ = bulk flow field ($\boldsymbol{v}^{\mathrm{T}}\boldsymbol{v} = 1$)

Tissue Properties from DCE-MRI Sequences

Dynamic Contrast Enhanced Magnetic Resonance Imaging (DCE-MRI): Varying the constrast helps to reveal possible pathology. [Video1] [Video2]

Goal: Estimate tissue transport properties to identify and to visualize pathology quantitatively:

$$\left\{\begin{array}{rcll} \partial_t C + \nabla\cdot(F\boldsymbol{v}) & = & \nabla\cdot(\mathcal{D}(\boldsymbol{v})\nabla C)\,, & \Omega\times(0,T] \\ \boldsymbol{n}\cdot(\mathcal{D}(\boldsymbol{v})\nabla C) & = & 0, & \Sigma\times(0,T] \\ C & = & C_{\mathrm{AIF}}, & \Gamma\times(0,T] \\ C & = & C_0, & \Omega\times\{t=0\} \end{array}\right.$$

$$\begin{array}{rcl} F & = & \text{mean velocity (perfusion)} \\ \boldsymbol{v} & = & \text{bulk flow field } (\boldsymbol{v}^{\mathrm{T}}\boldsymbol{v}=1) \\ \mathcal{D}(\boldsymbol{v}) & = & D\boldsymbol{v}\boldsymbol{v}^{\mathrm{T}} + P(I-\boldsymbol{v}\boldsymbol{v}^{\mathrm{T}}) \end{array}$$

Tissue Properties from DCE-MRI Sequences

Dynamic Contrast Enhanced Magnetic Resonance Imaging (DCE-MRI): Varying the constrast helps to reveal possible pathology. [Video1] [Video2]

Goal: Estimate tissue transport properties to identify and to visualize pathology quantitatively:

$$\begin{cases} \partial_t C + \nabla \cdot (F\boldsymbol{v}) = \nabla \cdot (\mathcal{D}(\boldsymbol{v})\nabla C), & \Omega \times (0, T] \\ \boldsymbol{n} \cdot (\mathcal{D}(\boldsymbol{v})\nabla C) = 0, & \Sigma \times (0, T] \\ C = C_{\mathrm{AIF}}, & \Gamma \times (0, T] \\ C = C_0, & \Omega \times \{t = 0\} \end{cases}$$

F = mean velocity (perfusion)

$\boldsymbol{v}$ = bulk flow field ($\boldsymbol{v}^{\mathrm{T}}\boldsymbol{v} = 1$)

$\mathcal{D}(\boldsymbol{v}) = D\boldsymbol{v}\boldsymbol{v}^{\mathrm{T}} + P(I - \boldsymbol{v}\boldsymbol{v}^{\mathrm{T}})$

D = streamline oriented diffusivity

Tissue Properties from DCE-MRI Sequences

Dynamic Contrast Enhanced Magnetic Resonance Imaging (DCE-MRI): Varying the constrast helps to reveal possible pathology. [Video1] [Video2]

Goal: Estimate tissue transport properties to identify and to visualize pathology quantitatively:

$$\left\{\begin{array}{rcll} \partial_t C + \nabla\cdot(F\boldsymbol{v}) &=& \nabla\cdot(\mathcal{D}(\boldsymbol{v})\nabla C)\,, & \Omega\times(0,T] \\ \boldsymbol{n}\cdot(\mathcal{D}(\boldsymbol{v})\nabla C) &=& 0, & \Sigma\times(0,T] \\ C &=& C_{\mathrm{AIF}}, & \Gamma\times(0,T] \\ C &=& C_0, & \Omega\times\{t=0\} \end{array}\right.$$

$$\begin{array}{rcl} F &=& \text{mean velocity (perfusion)} \\ \boldsymbol{v} &=& \text{bulk flow field } (\boldsymbol{v}^{\mathrm{T}}\boldsymbol{v}=1) \\ \mathcal{D}(\boldsymbol{v}) &=& D\boldsymbol{v}\boldsymbol{v}^{\mathrm{T}} + P(I-\boldsymbol{v}\boldsymbol{v}^{\mathrm{T}}) \\ D &=& \text{streamline oriented diffusivity} \\ P &=& \text{streamline orthogonal diffusivity (permeability)} \end{array}$$

Tissue Properties from DCE-MRI Sequences

Dynamic Contrast Enhanced Magnetic Resonance Imaging (DCE-MRI): Varying the constrast helps to reveal possible pathology. [Video1] [Video2]

Goal: Estimate tissue transport properties to identify and to visualize pathology quantitatively:

$$\begin{cases} \partial_t C + \nabla \cdot (F\boldsymbol{v}) & = & \nabla \cdot (\mathcal{D}(\boldsymbol{v})\nabla C)\,, & \Omega \times (0,T] \\ \boldsymbol{n} \cdot (\mathcal{D}(\boldsymbol{v})\nabla C) & = & 0, & \Sigma \times (0,T] \\ C & = & C_{\mathrm{AIF}}, & \Gamma \times (0,T] \\ C & = & C_0, & \Omega \times \{t = 0\} \end{cases}$$

$$\begin{array}{rcl} F & = & \text{mean velocity (perfusion)} \\ \boldsymbol{v} & = & \text{bulk flow field } (\boldsymbol{v}^{\mathrm{T}}\boldsymbol{v} = 1) \\ \mathcal{D}(\boldsymbol{v}) & = & D\boldsymbol{v}\boldsymbol{v}^{\mathrm{T}} + P(I - \boldsymbol{v}\boldsymbol{v}^{\mathrm{T}}) \\ D & = & \text{streamline oriented diffusivity} \\ P & = & \text{streamline orthogonal diffusivity (permeability)} \\ C_{\mathrm{AIF}} & = & \text{arterial input function} \end{array}$$

Tissue Properties from DCE-MRI Sequences

Simplified convolution model obtained through the semigroup:

$$C_{\mathrm{T}}(t) = \int_0^t K(t-s) C_{\mathrm{AIF}}(s) ds$$

Tissue Properties from DCE-MRI Sequences

Simplified convolution model obtained through the semigroup:

$$C_{\mathrm{T}}(t) = \int_0^t K(t-s) C_{\mathrm{AIF}}(s) ds$$

where

$$C_{\mathrm{T}}(t) = \frac{1}{|\Omega|} \int_{\Omega} C(\boldsymbol{x}, t) d\boldsymbol{x}, \quad K(t) = \frac{1}{|\Omega|} \int_{\Omega} AS(t) I_{\Omega}(\boldsymbol{x}) d\boldsymbol{x}$$

Tissue Properties from DCE-MRI Sequences

Simplified convolution model obtained through the semigroup:

$$C_{\mathrm{T}}(t) = \int_0^t K(t-s) C_{\mathrm{AIF}}(s) ds$$

where

$$C_{\mathrm{T}}(t) = \frac{1}{|\Omega|} \int_{\Omega} C(\boldsymbol{x}, t) d\boldsymbol{x}, \quad K(t) = \frac{1}{|\Omega|} \int_{\Omega} AS(t) I_{\Omega}(\boldsymbol{x}) d\boldsymbol{x}$$

Physiological parameters:

flow rate per unit volume $\mathcal{F}_{\mathrm{T}} \quad = \quad K(0)$

Tissue Properties from DCE-MRI Sequences

Simplified convolution model obtained through the semigroup:

$$C_{\mathrm{T}}(t) = \int_0^t K(t-s)C_{\mathrm{AIF}}(s)ds$$

where

$$C_{\mathrm{T}}(t) = \frac{1}{|\Omega|}\int_\Omega C(\boldsymbol{x},t)d\boldsymbol{x}, \quad K(t) = \frac{1}{|\Omega|}\int_\Omega AS(t)I_\Omega(\boldsymbol{x})d\boldsymbol{x}$$

Physiological parameters:

$$\begin{aligned} \text{flow rate per unit volume } \mathcal{F}_{\mathrm{T}} &= K(0) \\ \text{volume fraction } \mathcal{V}_{\mathrm{T}} &= \int_0^T K(t)dt \end{aligned}$$

Tissue Properties from DCE-MRI Sequences

Simplified convolution model obtained through the semigroup:

$$C_{\mathrm{T}}(t) = \int_0^t K(t-s) C_{\mathrm{AIF}}(s) ds$$

where

$$C_{\mathrm{T}}(t) = \frac{1}{|\Omega|} \int_\Omega C(\boldsymbol{x}, t) d\boldsymbol{x}, \quad K(t) = \frac{1}{|\Omega|} \int_\Omega AS(t) I_\Omega(\boldsymbol{x}) d\boldsymbol{x}$$

Physiological parameters:

$$\begin{aligned}
\text{flow rate per unit volume } \mathcal{F}_{\mathrm{T}} &= K(0) \\
\text{volume fraction } \mathcal{V}_{\mathrm{T}} &= \int_0^T K(t) dt \\
\text{mean transit time } \mathcal{T}_{\mathrm{T}} &= \int_0^T K(t)/K(0) dt
\end{aligned}$$

Tissue Properties from DCE-MRI Sequences

Proposed deconvolution approach:

Tissue Properties from DCE-MRI Sequences

Proposed deconvolution approach: An exponential basis arises naturally from compartmental analysis in physiology.

$$K(t) \approx \sum_{m=1}^{M} k_m e^{-\lambda_m t}$$

Tissue Properties from DCE-MRI Sequences

Proposed deconvolution approach: An exponential basis arises naturally from compartmental analysis in physiology.

$$K(t) \approx \sum_{m=1}^{M} k_m e^{-\lambda_m t}$$

Practitioners: $M = 2$! but $\lambda_m = ?$

Tissue Properties from DCE-MRI Sequences

Proposed deconvolution approach: An exponential basis arises naturally from compartmental analysis in physiology.

$$K(t) \approx \sum_{m=1}^{M} k_m e^{-\lambda_m t}$$

Practitioners: $M = 2$! but $\lambda_m = ?$
Theoreticians: (Müntz Theorem) $\{e^{\lambda_m t}\}$ dense in $L^2[0, \infty)$ if

$$\lim_{m \to \infty} \lambda_m = \infty = \sum_{m=1}^{\infty} \lambda_m^{-1}$$

Tissue Properties from DCE-MRI Sequences

Proposed deconvolution approach: An exponential basis arises naturally from compartmental analysis in physiology.

$$K(t) \approx \sum_{m=1}^{M} k_m e^{-\lambda_m t}$$

Practitioners: $M = 2$! but $\lambda_m = ?$
Theoreticians: (Müntz Theorem) $\{e^{\lambda_m t}\}$ dense in $L^2[0, \infty)$ if

$$\lim_{m \to \infty} \lambda_m = \infty = \sum_{m=1}^{\infty} \lambda_m^{-1}$$

Take time scales harmonically distributed: $\lambda_m^{-1} = T/m$

Tissue Properties from DCE-MRI Sequences

Proposed deconvolution approach: An exponential basis arises naturally from compartmental analysis in physiology.

$$K(t) \approx \sum_{m=1}^{M} k_m e^{-\lambda_m t}$$

Practitioners: $M = 2$! but $\lambda_m = ?$
Theoreticians: (Müntz Theorem) $\{e^{\lambda_m t}\}$ dense in $L^2[0, \infty)$ if

$$\lim_{m \to \infty} \lambda_m = \infty = \sum_{m=1}^{\infty} \lambda_m^{-1}$$

Take time scales harmonically distributed: $\lambda_m^{-1} = T/m$

Constrain K to be decreasing: $\boldsymbol{k}^{\mathrm{T}}[\Lambda D_1^{-1} \cdots D_M^{-1}] \geq 0$

Tissue Properties from DCE-MRI Sequences

Proposed deconvolution approach: An exponential basis arises naturally from compartmental analysis in physiology.

$$K(t) \approx \sum_{m=1}^{M} k_m e^{-\lambda_m t}$$

Practitioners: $M = 2$! but $\lambda_m = ?$
Theoreticians: (Müntz Theorem) $\{e^{\lambda_m t}\}$ dense in $L^2[0,\infty)$ if

$$\lim_{m\to\infty} \lambda_m = \infty = \sum_{m=1}^{\infty} \lambda_m^{-1}$$

Take time scales harmonically distributed: $\lambda_m^{-1} = T/m$

Constrain K to be decreasing: $\boldsymbol{k}^{\mathrm{T}}[\Lambda D_1^{-1} \cdots D_M^{-1}] \geq 0$ where $\{D_m\}$ depend upon $\{(\lambda_i - \lambda_j)^{-l}, 1 \leq i, j \leq M, l = 0, \ldots, M\}$.

Tissue Properties from DCE-MRI Sequences

Application to measured data:

singular value decomposition | constrained splines | constrained exponentials

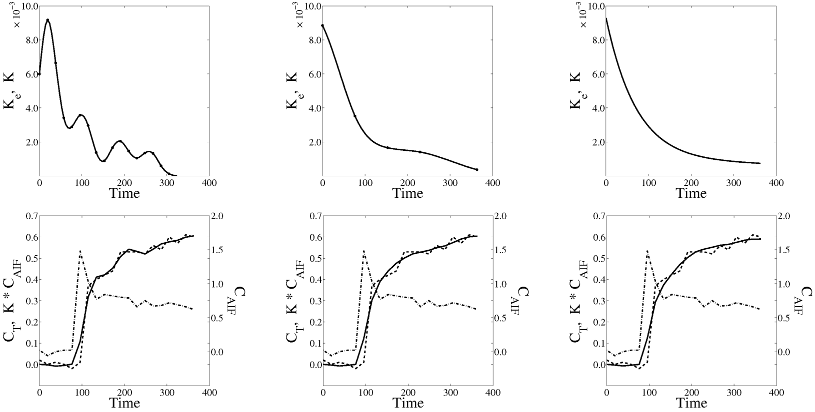

Tissue Properties from DCE-MRI Sequences

Pixelwise comparison of EXP (top row) and SVD (bottom row)

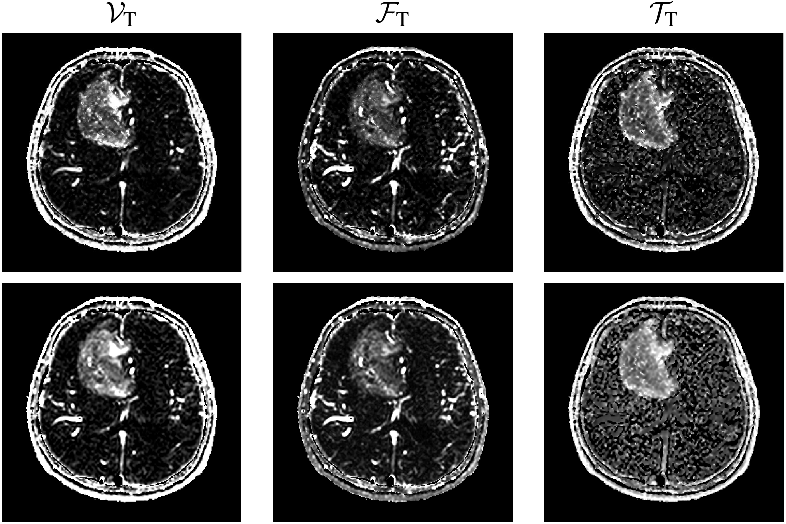

Image Reconstruction for Parallel Imaging

Goal: Obtain high temporal resolution for DCE-MRI through acceleration of data acquisition.

Image Reconstruction for Parallel Imaging

Goal: Obtain high temporal resolution for DCE-MRI through acceleration of data acquisition.

Strategy: Undersampling. Disadvantage: Images are distorted. Distortions must be corrected.

Image Reconstruction for Parallel Imaging

Goal: Obtain high temporal resolution for DCE-MRI through acceleration of data acquisition.

Strategy: Undersampling. Disadvantage: Images are distorted. Distortions must be corrected.

The Hardware:

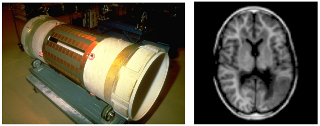

usual coil

Image Reconstruction for Parallel Imaging

Goal: Obtain high temporal resolution for DCE-MRI through acceleration of data acquisition.

Strategy: Undersampling. Disadvantage: Images are distorted. Distortions must be corrected.

The Hardware:

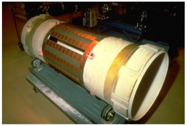

usual coil

smaller coils

The smaller coils measure in parallel with complementary subsampling, but their images are

Image Reconstruction for Parallel Imaging

Goal: Obtain high temporal resolution for DCE-MRI through acceleration of data acquisition.

Strategy: Undersampling. Disadvantage: Images are distorted. Distortions must be corrected.

The Hardware:

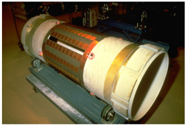


usual coil


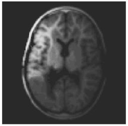

smaller coils

The smaller coils measure in parallel with complementary subsampling, but their images are modulated

Image Reconstruction for Parallel Imaging

Goal: Obtain high temporal resolution for DCE-MRI through acceleration of data acquisition.

Strategy: Undersampling. Disadvantage: Images are distorted. Distortions must be corrected.

The Hardware:

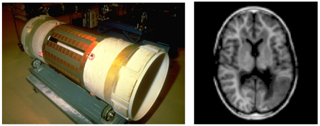

usual coil

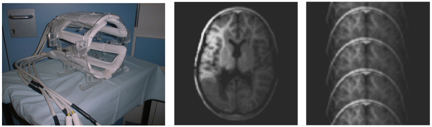

smaller coils

The smaller coils measure in parallel with complementary subsampling, but their images are modulated *and* aliased.

Image Reconstruction for Parallel Imaging

Goal: Obtain high temporal resolution for DCE-MRI through acceleration of data acquisition.

Strategy: Undersampling. Disadvantage: Images are distorted. Distortions must be corrected.

The Hardware:

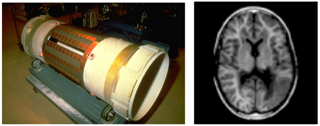

usual coil

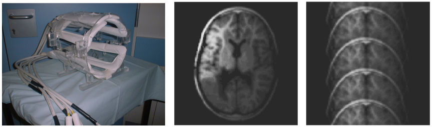

smaller coils

The smaller coils measure in parallel with complementary subsampling, but their images are modulated *and* aliased.

For Cartesian subsampling aliasing is structured not noise-like.

Image Reconstruction for Parallel Imaging

Through Minimization of the functional:

$$J(I,\sigma_i) = \sum_i \int_\Omega |P(\sigma_i I) - I_i|^2 + \nu \int_\Omega |D^2\sigma_i|^2 + \kappa \int_\Omega |I|^2 + \mu \int_\Omega \phi_\epsilon(|DI|)$$

Image Reconstruction for Parallel Imaging

Through Minimization of the functional:

$$J(I,\sigma_i) = \sum_i \int_\Omega |P(\sigma_i I) - I_i|^2 + \nu \int_\Omega |D^2 \sigma_i|^2 + \kappa \int_\Omega |I|^2 + \mu \int_\Omega \phi_\epsilon(|DI|)$$

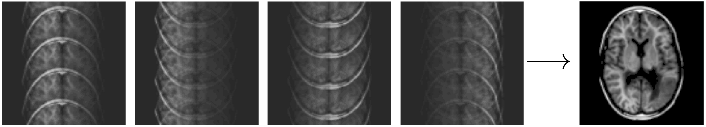

modulated und aliased reconstructed

Image Reconstruction for Parallel Imaging

Through Minimization of the functional:

$$J(I,\sigma_i) = \sum_i \int_\Omega |P(\sigma_i I) - I_i|^2 + \nu \int_\Omega |D^2 \sigma_i|^2 + \kappa \int_\Omega |I|^2 + \mu \int_\Omega \phi_\epsilon(|DI|)$$

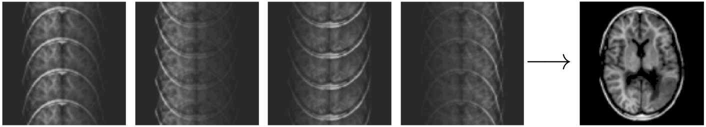

modulated und aliased reconstructed

Optimality System: biharmonic for σ_i,

$$\left[\nu \Delta^2 + I^* P I\right] \sigma_i = I^* I_i,$$

Image Reconstruction for Parallel Imaging

Through Minimization of the functional:

$$J(I,\sigma_i) = \sum_i \int_\Omega |P(\sigma_i I) - I_i|^2 + \nu \int_\Omega |D^2\sigma_i|^2 + \kappa \int_\Omega |I|^2 + \mu \int_\Omega \phi_\epsilon(|DI|)$$

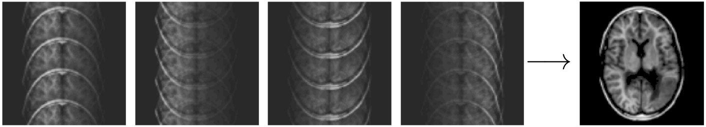

modulated und aliased reconstructed

Optimality System: biharmonic for σ_i, primal-dual for I

$$\left[\nu\Delta^2 + I^* P I\right]\sigma_i = I^* I_i, \quad \lfloor \nabla I \rfloor_\epsilon = \max\{\epsilon, |\nabla I|\}$$

$$\left[\kappa + \sum_i \sigma_i^* P \sigma_i\right] I + \nabla \cdot \boldsymbol{p} = \sum_i \sigma_i^* I_i, \quad -\mu \nabla I + \lfloor \nabla I \rfloor_\epsilon \boldsymbol{p} = 0$$

Image Reconstruction for Parallel Imaging

Through Minimization of the functional:

$$J(I,\sigma_i) = \sum_i \int_\Omega |P(\sigma_i I) - I_i|^2 + \nu \int_\Omega |D^2 \sigma_i|^2 + \kappa \int_\Omega |I|^2 + \mu \int_\Omega \phi_\epsilon(|DI|)$$

Optimality System: biharmonic for σ_i, primal-dual for I

$$\left[\nu \Delta^2 + I^* P I\right] \sigma_i = I^* I_i, \quad \lfloor \nabla I \rfloor_\epsilon = \max\{\epsilon, |\nabla I|\}$$

$$\left[\kappa + \sum_i \sigma_i^* P \sigma_i\right] I + \nabla \cdot \boldsymbol{p} = \sum_i \sigma_i^* I_i, \quad -\mu \nabla I + \lfloor \nabla I \rfloor_\epsilon \boldsymbol{p} = 0$$

Image Reconstruction for Parallel Imaging

Through Minimization of the functional:

$$J(I,\sigma_i) = \sum_i \int_\Omega |P(\sigma_i I) - I_i|^2 + \nu \int_\Omega |D^2\sigma_i|^2 + \kappa \int_\Omega |I|^2 + \mu \int_\Omega \phi_\epsilon(|DI|)$$

Optimality System: biharmonic for σ_i, primal-dual for I

$$\left[\nu\Delta^2 + I^* P I\right]\sigma_i = I^* I_i, \quad \lfloor \nabla I \rfloor_\epsilon = \max\{\epsilon, |\nabla I|\}$$

$$\left[\kappa + \sum_i \sigma_i^* P \sigma_i\right] I + \nabla \cdot \boldsymbol{p} = \sum_i \sigma_i^* I_i, \quad -\mu\nabla I + \lfloor \nabla I \rfloor_\epsilon \boldsymbol{p} = 0$$

- Solved by a Newton's Method with projection:

$$\|I\|_{L^2}^2 = N_\mathrm{a} \sum_i \|I_i\|_{L^2}^2$$

Image Reconstruction for Parallel Imaging

Through Minimization of the functional:

$$J(I,\sigma_i) = \sum_i \int_\Omega |P(\sigma_i I) - I_i|^2 + \nu \int_\Omega |D^2\sigma_i|^2 + \kappa \int_\Omega |I|^2 + \mu \int_\Omega \phi_\epsilon(|DI|)$$

Optimality System: biharmonic for σ_i, primal-dual for I

$$\left[\nu\Delta^2 + I^* P I\right]\sigma_i = I^* I_i, \quad \lfloor \nabla I \rfloor_\epsilon = \max\{\epsilon, |\nabla I|\}$$

$$\left[\kappa + \sum_i \sigma_i^* P \sigma_i\right] I + \nabla \cdot \boldsymbol{p} = \sum_i \sigma_i^* I_i, \quad -\mu \nabla I + \lfloor \nabla I \rfloor_\epsilon \boldsymbol{p} = 0$$

- Solved by a Newton's Method with projection:

$$\|I\|_{L^2}^2 = N_{\mathrm{a}} \sum_i \|I_i\|_{L^2}^2$$

- Spectral approaches impose unnatural periodic BCs.

Image Reconstruction for Parallel Imaging

Comparison of methods:

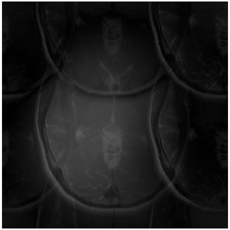

Data

- Data are highly undersampled in both directions.

Image Reconstruction for Parallel Imaging

Comparison of methods:

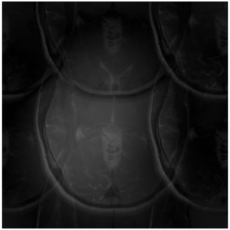

Data

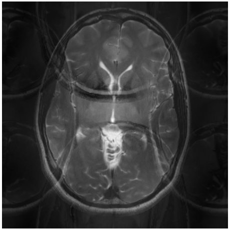

GRAPPA

- GRAPPA [Griswold et al.] in Siemens equipment.

Image Reconstruction for Parallel Imaging

Comparison of methods:

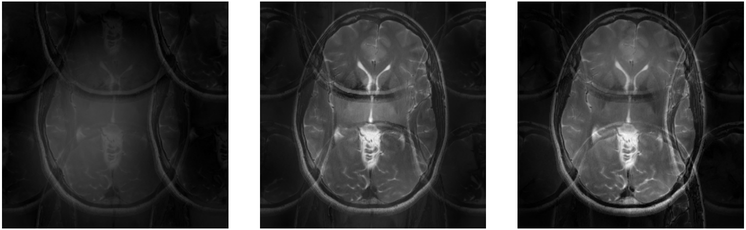

Data GRAPPA SENSE

- SENSE [Pruesmann et al.] in Philips equipment.

Image Reconstruction for Parallel Imaging

Comparison of methods:

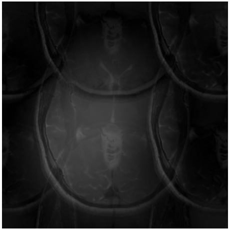

Data

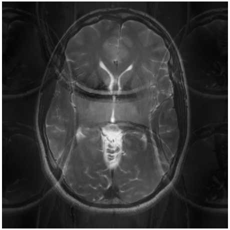

GRAPPA

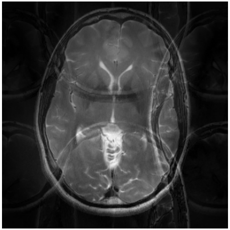

SENSE

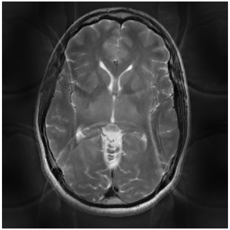

IRGN

- IRGN [Uecker et al.] from Göttingen.

Image Reconstruction for Parallel Imaging

Comparison of methods:

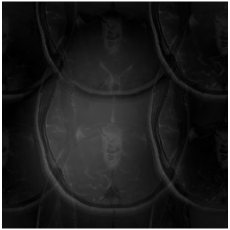

Data

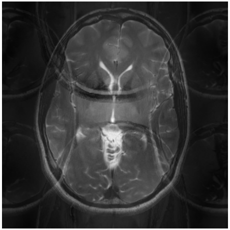

GRAPPA

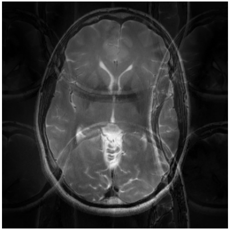

SENSE

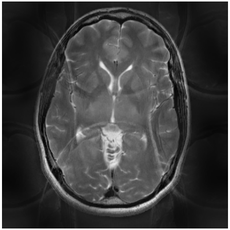

IRGN

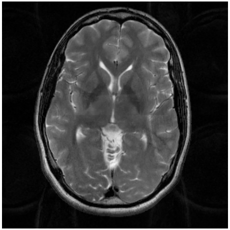

TVSENSE

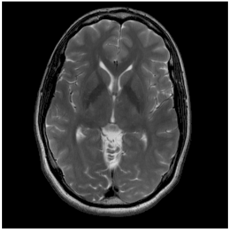

Exact

- TVSENSE [Keeling et al.] from Graz.

Registration of DCE-MRI Sequences

Example: [Video]

Objective: Remove the motion in a DCE-MRI sequence so that individual tissue points can be investigated.

Registration of DCE-MRI Sequences

Example: [Video]

Objective: Remove the motion in a DCE-MRI sequence so that individual tissue points can be investigated.

Plan A: Register all images to a fixed target.

Registration of DCE-MRI Sequences

Example: [Video]

Challenges for an image similarity measure:

- Higher contrast creates new structures (edge based?)
- Intensities change within the sequence (intensity based?)
- Gradual intensity variations within single images (segmentation based?)

Image Similarity Measures for DCE-MRI

Higher contrast creates new structures:

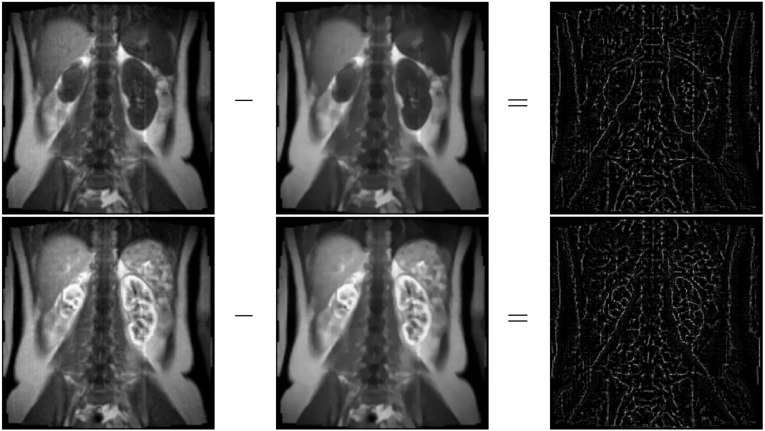

Original − TV smoothed = texture

Edge based similarity measure?

Image Similarity Measures for DCE-MRI

Higher contrast creates new structures:

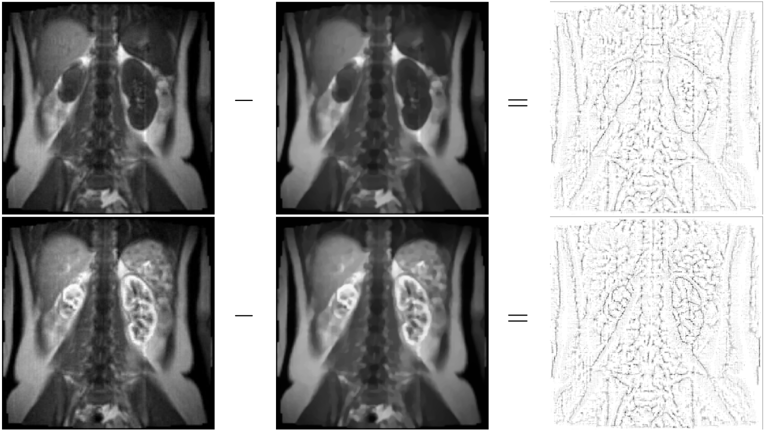

Original − TV smoothed = texture

Edge based similarity measure?

Image Similarity Measures for DCE-MRI

Intensities change within the sequence:

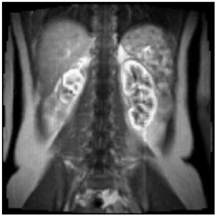

$-$

$=$

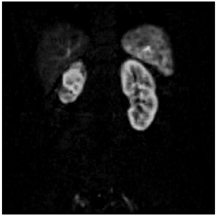

I_1 I_0 $I_1 - I_0$

Here the patient at I_0 is a trivial displacement of the patient at I_1.

Intensity based similarity measure?

Image Similarity Measures for DCE-MRI

Gradual intensity variations within single images:

original images

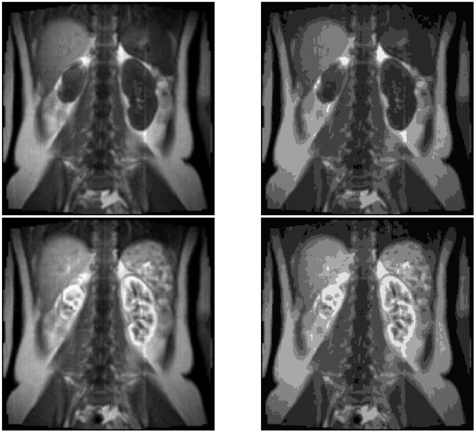

piecewise constant segmentations

Segmentation based similarity measure?

Explicit Similarity Measures

For Sum of Squared Differences,

$$S(I_0, I_1, u) = \int_\Omega |I_0 \circ (\mathrm{Id} + u) - I_1|^2$$

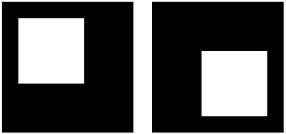

Explicit Similarity Measures

For Sum of Squared Differences,

$$S(I_0, I_1, u) = \int_\Omega |I_0 \circ (\mathrm{Id} + u) - I_1|^2$$

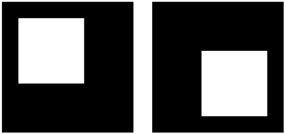

Force field in the optimality system:

vertical component: 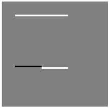

horizontal component: 

Explicit Similarity Measures

For Sum of Squared Differences,

$$S(I_0, I_1, u) = \int_\Omega |I_0 \circ (\mathrm{Id} + u) - I_1|^2$$

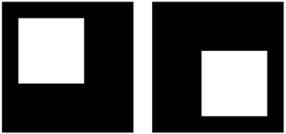

Force field in the optimality system:

vertical component:

horizontal component:

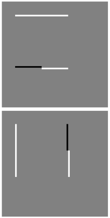

stronger still for *symmetric* sum of squared differences

Explicit Similarity Measures

For an edge based measure, e.g.,

$$S(I_0, I_1, u) = \int_\Omega |n_0 \circ (\mathrm{Id} + u) \times n_1|^2, \quad n_k = \nabla I_k / |\nabla I_k|$$

Explicit Similarity Measures

For an edge based measure, e.g.,

$$S(I_0, I_1, u) = \int_\Omega |n_0 \circ (\mathrm{Id} + u) \times n_1|^2, \quad n_k = \nabla I_k / |\nabla I_k|$$

Force field in the optimality system:

vertical component: 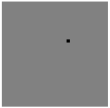

horizontal component: 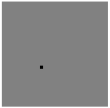

Explicit Similarity Measures

For an edge based measure, e.g.,

$$S(I_0, I_1, u) = \int_\Omega |n_0 \circ (\mathrm{Id} + u) \times n_1|^2, \quad n_k = \nabla I_k / |\nabla I_k|$$

Further, $I_0 \circ (\mathrm{Id} + u)$ must start very close to I_1 for correct convergence

Force field in the optimality system:

vertical component:

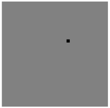

horizontal component:

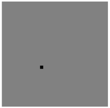

Explicit Similarity Measures

Proposed Rescaling Measure:

$$S(I_0, I_1, u) = \int_\Omega |I_0 \circ (\mathrm{Id} + u) - R[I_1]|^2$$

Explicit Similarity Measures

Proposed Rescaling Measure:

$$S(I_0, I_1, u) = \int_\Omega |I_0 \circ (\mathrm{Id} + u) - R[I_1]|^2$$

where R is a local rescaling of intensities:

$$R[I_1] = \sum_{\omega \subset \mathcal{S}_d(I_1)} p_\omega \chi_\omega, \quad p_\omega = \arg\min_{p \in \mathcal{P}^d} \int_\omega |I_0 \circ (\mathrm{Id} + u) - p|^2$$

Explicit Similarity Measures

Proposed Rescaling Measure:

$$S(I_0, I_1, u) = \int_\Omega |I_0 \circ (\mathrm{Id} + u) - R[I_1]|^2$$

where R is a local rescaling of intensities:

$$R[I_1] = \sum_{\omega \subset \mathcal{S}_d(I_1)} p_\omega \chi_\omega, \quad p_\omega = \arg\min_{p \in \mathcal{P}^d} \int_\omega |I_0 \circ (\mathrm{Id} + u) - p|^2$$

and $\mathcal{S}_d(I_1)$ is a dth degree segmentation of I_1: conn($\{\omega_m\}$)

$$\sum_{m=1}^{M} \int_{\omega_m} |q_m - I_1|^2 = \min \left\{ \{q_m\} \subset \mathcal{P}^d, \omega_m \cap \omega_n = \emptyset, \Omega = \bigcup_{m=1}^{M} \omega_m \right\}$$

Explicit Similarity Measures

Proposed Rescaling Measure:

$$S(I_0, I_1, u) = \int_\Omega |I_0 \circ (\mathrm{Id} + u) - R[I_1]|^2$$

where R is a local rescaling of intensities:

$$R[I_1] = \sum_{\omega \subset \mathcal{S}_d(I_1)} p_\omega \chi_\omega, \quad p_\omega = \arg\min_{p \in \mathcal{P}^d} \int_\omega |I_0 \circ (\mathrm{Id} + u) - p|^2$$

and $\mathcal{S}_d(I_1)$ is a dth degree segmentation of I_1: $\mathrm{conn}(\{\omega_m\})$

$$\sum_{m=1}^{M} \int_{\omega_m} |q_m - I_1|^2 = \min \left\{ \{q_m\} \subset \mathcal{P}^d, \omega_m \cap \omega_n = \emptyset, \Omega = \bigcup_{m=1}^{M} \omega_m \right\}$$

an approximation to a higher order Mumford Shah functional:

$$\min_{I,\Gamma} = \int_\Omega |I - I_1|^2 + \alpha \int_{\Omega \setminus \Gamma} |\nabla^{d+1} I|^2 + \beta |\Gamma|$$

Segmentation of Degree *d* in 1D

Initial

Final

Constant

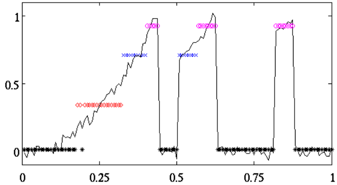

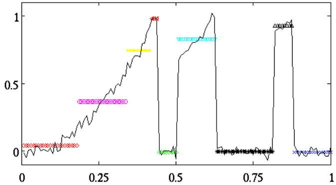

Segmentation of Degree *d* in 1D

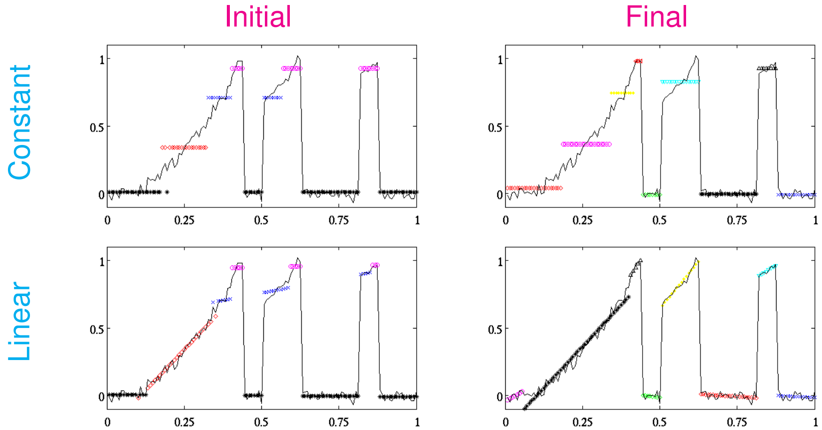

Segmentation of Degree *d* in 1D

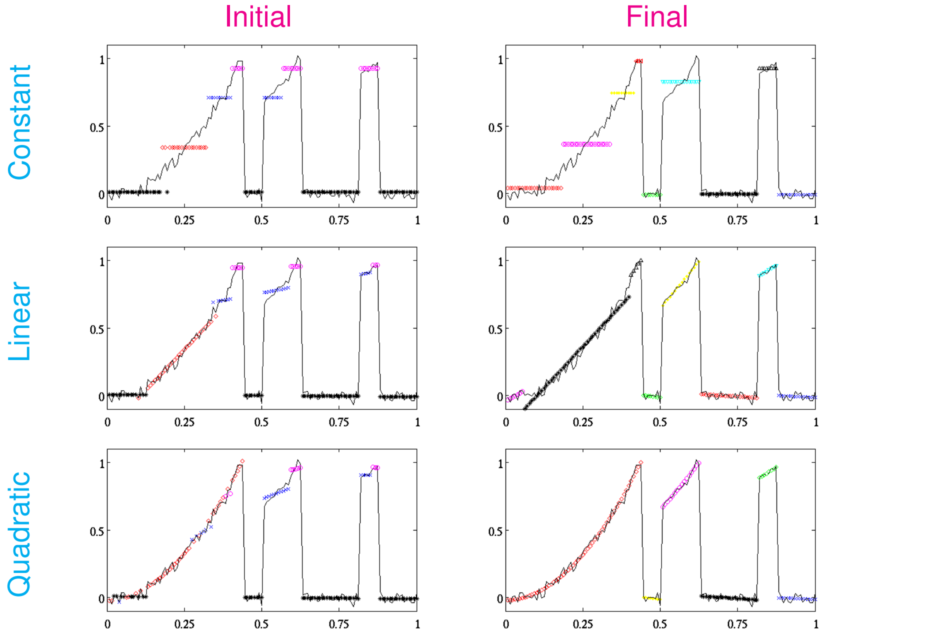

Computation of Segmentation of Degree d

Initially: Minimize

$$\sum_{m=1}^{M} \int_{\omega_m} |q_m - I|^2 \quad \text{over} \quad \left\{ \{q_m\} \subset \mathcal{P}^d, \omega_m \cap \omega_n = \emptyset, \Omega = \bigcup_{m=1}^{M} \omega_m \right\}$$

Computation of Segmentation of Degree d

Initially: Minimize

$$\sum_{m=1}^{M} \int_{\omega_m} |q_m - I|^2 \quad \text{over} \quad \left\{ \{q_m\} \subset \mathcal{P}^d, \omega_m \cap \omega_n = \emptyset, \Omega = \bigcup_{m=1}^{M} \omega_m \right\}$$

then grow conn($\{\omega_m\}$) according to:

$$\partial\omega \ni x \to \omega : |p_\omega(x) - I(x)| \leq \gamma \sqrt{\sigma_\omega}$$

Computation of Segmentation of Degree d

Initially: Minimize

$$\sum_{m=1}^{M} \int_{\omega_m} |q_m - I|^2 \quad \text{over} \quad \left\{ \{q_m\} \subset \mathcal{P}^d, \omega_m \cap \omega_n = \emptyset, \Omega = \bigcup_{m=1}^{M} \omega_m \right\}$$

then grow conn($\{\omega_m\}$) according to:

$$\partial\omega \ni x \to \omega : |p_\omega(x) - I(x)| \leq \gamma\sqrt{\sigma_\omega}$$

Finally: Minimize an approximation to the functional:

$$\min_{I,\Gamma} = \int_\Omega |I - I_1|^2 + \alpha \int_{\Omega\setminus\Gamma} |\nabla^{d+1} I|^2 + \beta|\Gamma|$$

discussed below.

Segmentation of Degree d in 2D

original

Segmentation of Degree d in 2D

original

piecewise constant

Segmentation of Degree d in 2D

original

piecewise constant

piecewise linear

Segmentation of Degree d in 2D

original

piecewise constant

piecewise linear

piecewise quadratic

Explicit Similarity Measures

When Segmentation and Registration performed *sequentially*:

- Higher degree models adapt intensities *too* well,
- and the force driving registration is *too* low.

Explicit Similarity Measures

When Segmentation and Registration performed *sequentially*:

- Higher degree models adapt intensities *too* well,
- and the force driving registration is *too* low.

Thus, the Rescaling Measure is taken as:

$$S(I_0, I_1, u) = \int_\Omega |I_0 \circ (\mathrm{Id} + u) - R[I_1]|^2$$

where R is a local rescaling of intensities:

$$R[I_1](\omega) = I_1(\omega) + \fint_\omega [I_0 \circ (\mathrm{Id} + u) - I_1] \quad \omega \subset \mathcal{S}_d(I_1)$$

where $\mathcal{S}_d(I_1)$ is a $d = 0$th degree segmentation of I_1.

Explicit Similarity Measures

When Segmentation and Registration performed *sequentially*:

- Higher degree models adapt intensities *too* well,
- and the force driving registration is *too* low.

Thus, the Rescaling Measure is taken as:

$$S(I_0, I_1, u) = \int_\Omega |I_0 \circ (\mathrm{Id} + u) - R[I_1]|^2$$

where R is a local rescaling of intensities:

$$R[I_1](\omega) = I_1(\omega) + \fint_\omega [I_0 \circ (\mathrm{Id} + u) - I_1] \quad \omega \subset \mathcal{S}_d(I_1)$$

where $\mathcal{S}_d(I_1)$ is a $d = 0$th degree segmentation of I_1.

[Video]

Registration Regularization

Pairwise registration accomplished by minimizing

$$J(u) = S(I_0, I_1, u) + E(u)$$

with the rescaling similarity measure,

$$S(I_0, I_1, u) = \int_\Omega |I_0 \circ (\mathrm{Id} + u) - R[I_1]|^2$$

and linear elastic energy,

$$E(u) = \int_\Omega \left\{ \lambda |\nabla \cdot u|^2 + \tfrac{1}{2}\mu |\nabla u^{\mathrm{T}} + \nabla u|^2 \right\}$$

Registration Regularization

Pairwise registration accomplished by minimizing

$$J(u) = S(I_0, I_1, u) + E(u)$$

with the rescaling similarity measure,

$$S(I_0, I_1, u) = \int_\Omega |I_0 \circ (\mathrm{Id} + u) - R[I_1]|^2$$

and linear elastic energy,

$$E(u) = \int_\Omega \left\{ \lambda |\nabla \cdot u|^2 + \tfrac{1}{2}\mu |\nabla u^{\mathrm{T}} + \nabla u|^2 \right\}$$

With [Fürtinger]: Existence of Minimizers for $J(u)$.

Registration Regularization

Pairwise registration accomplished by minimizing

$$J(u) = S(I_0, I_1, u) + E(u)$$

with the rescaling similarity measure,

$$S(I_0, I_1, u) = \int_\Omega |I_0 \circ (\mathrm{Id} + u) - R[I_1]|^2$$

and linear elastic energy,

$$E(u) = \int_\Omega \left\{ \lambda |\nabla \cdot u|^2 + \frac{1}{2}\mu |\nabla u^{\mathrm{T}} + \nabla u|^2 \right\}$$

With [Fürtinger]: Existence of Minimizers for $J(u)$.

Optimality system solved by Newton's method with line search.

Registration Result

An image pair at the arrival moment of contrast agent:

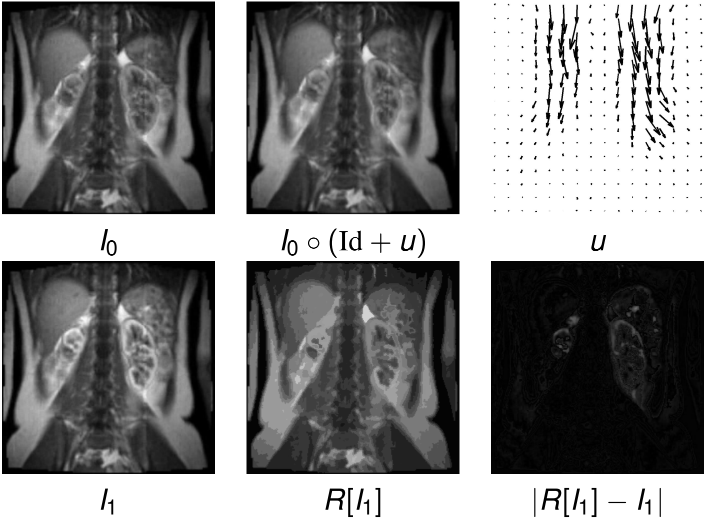

Result ($d = 0$) superior to those with TV regularization: [Video].

Kidneys are particularly motionless.

Higher Order Models: Total Generalized Variation

Goal: Overcome the essentially piecewise constant model of TV regularization.

Higher Order Models: Total Generalized Variation

Goal: Overcome the essentially piecewise constant model of TV regularization. In the classical approach, minimize:

$$J(I) = \int_\Omega |I - \tilde{I}|^2 + \mathrm{TV}_\alpha(I)$$

Higher Order Models: Total Generalized Variation

Goal: Overcome the essentially piecewise constant model of TV regularization. In the classical approach, minimize:

$$J(I) = \int_\Omega |I - \tilde{I}|^2 + \mathrm{TV}_\alpha(I) \qquad \text{where}$$

$$\alpha \int_\Omega |DI| = \mathrm{TV}_\alpha(I) = \sup \left\{ \int_\Omega I \,\mathrm{div}\, \boldsymbol{\psi} : \|\boldsymbol{\psi}\|_\infty \leq \alpha, \boldsymbol{\psi} \in C_0^1(\Omega, \mathbb{R}^n) \right\}$$

Higher Order Models: Total Generalized Variation

Goal: Overcome the essentially piecewise constant model of TV regularization. In the classical approach, minimize:

$$J(I) = \int_\Omega |I - \tilde{I}|^2 + \mathrm{TV}_\alpha(I) \qquad \text{where}$$

$$\alpha \int_\Omega |DI| = \mathrm{TV}_\alpha(I) = \sup \left\{ \int_\Omega I \operatorname{div} \psi : \|\psi\|_\infty \leq \alpha, \psi \in C_0^1(\Omega, \mathbb{R}^n) \right\}$$

Noisy and TV-reconstructed images:

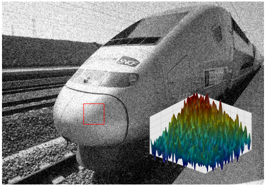

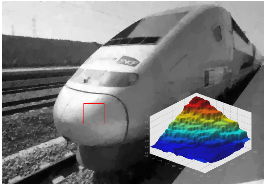

Higher Order Models: Total Generalized Variation

Goal: Develop a functional with a kernel which is richer than piecewise constants.

Higher Order Models: Total Generalized Variation

Goal: Develop a functional with a kernel which is richer than piecewise constants. In the generalized approach, minimize:

$$J(I) = \int_{\Omega} |I - \tilde{I}|^2 + \mathrm{TGV}_{\alpha}^{k}(I)$$

Higher Order Models: Total Generalized Variation

Goal: Develop a functional with a kernel which is richer than piecewise constants. In the generalized approach, minimize:

$$J(I) = \int_\Omega |I - \tilde{I}|^2 + \mathrm{TGV}_\alpha^k(I) \qquad \text{where}$$

$$\mathrm{TGV}_\alpha^k(I) = \sup\left\{\int_\Omega I \,\mathrm{div}^k \psi : \underbrace{\|\mathrm{div}^l \psi\|_\infty \le \alpha_l}_{l=0,\dots,k-1}, \psi \in C_0^k(\Omega, \mathrm{Sym}^k(\mathbb{R}^n))\right\}$$

Higher Order Models: Total Generalized Variation

Goal: Develop a functional with a kernel which is richer than piecewise constants. In the generalized approach, minimize:

$$J(I) = \int_\Omega |I - \tilde{I}|^2 + \mathrm{TGV}_\alpha^k(I) \qquad \text{where}$$

$$\mathrm{TGV}_\alpha^k(I) = \sup \left\{ \int_\Omega I \,\mathrm{div}^k \psi : \underbrace{\|\mathrm{div}^l \psi\|_\infty \leq \alpha_l}_{l=0,\ldots,k-1}, \psi \in C_0^k(\Omega, \mathrm{Sym}^k(\mathbb{R}^n)) \right\}$$

Noisy and TGV_α^2-reconstructed images: [Bredies, Kunisch, Pock]

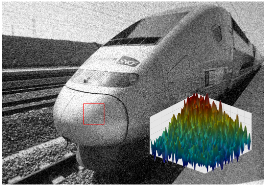

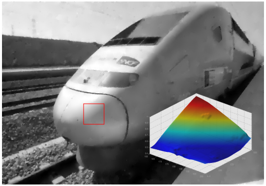

Higher Order Segmentation

Forthcoming results with [Fürtinger]: Higher order Mumford Shah,

$$\min_{I,\Gamma} = \int_\Omega |I - \tilde{I}|^2 + \alpha \int_{\Omega \setminus \Gamma} |\nabla^{d+1} I|^2 + \beta |\Gamma|$$

Higher Order Segmentation

Forthcoming results with [Fürtinger]: Higher order Mumford Shah,

$$\min_{I,\Gamma} = \int_{\Omega} |I - \tilde{I}|^2 + \alpha \int_{\Omega \setminus \Gamma} |\nabla^{d+1} I|^2 + \beta |\Gamma|$$

Phase function (Ambrosio-Tortorelli) approximation:

$$\min_{I,\phi} = \int_{\Omega} \left\{ |I - \tilde{I}|^2 + \alpha |\nabla^{d+1} I|^2 \phi^2 + \epsilon |\nabla \phi|^2 + \epsilon^{-1} |1 - \phi|^2 \right\}$$

but ϕ is drawn to zero by varying strengths of discrete $|\nabla^{d+1} I|^2$.

Higher Order Segmentation

Forthcoming results with [Fürtinger]: Higher order Mumford Shah,

$$\min_{I,\Gamma} = \int_\Omega |I - \tilde{I}|^2 + \alpha \int_{\Omega\setminus\Gamma} |\nabla^{d+1} I|^2 + \beta|\Gamma|$$

Phase function (Ambrosio-Tortorelli) approximation:

$$\min_{I,\phi} = \int_\Omega \left\{ |I - \tilde{I}|^2 + \alpha|\nabla^{d+1} I|^2 \phi^2 + \epsilon|\nabla\phi|^2 + \epsilon^{-1}|1-\phi|^2 \right\}$$

but ϕ is drawn to zero by varying strengths of discrete $|\nabla^{d+1} I|^2$.
Partition approximation: $I \to \sum_{m=1}^{M} c_m \chi_m$ ($M \leq 4$, 4CMT)

Higher Order Segmentation

Forthcoming results with [Fürtinger]: Higher order Mumford Shah,

$$\min_{I,\Gamma} = \int_\Omega |I - \tilde{I}|^2 + \alpha \int_{\Omega\setminus\Gamma} |\nabla^{d+1} I|^2 + \beta|\Gamma|$$

Phase function (Ambrosio-Tortorelli) approximation:

$$\min_{I,\phi} = \int_\Omega \left\{ |I - \tilde{I}|^2 + \alpha |\nabla^{d+1} I|^2 \phi^2 + \epsilon |\nabla \phi|^2 + \epsilon^{-1} |1 - \phi|^2 \right\}$$

but ϕ is drawn to zero by varying strengths of discrete $|\nabla^{d+1} I|^2$.
Partition approximation: $I \to \sum_{m=1}^{M} c_m \chi_m$ ($M \leq 4$, 4CMT)

$$\min_{c_m,\chi_m} = \int_\Omega \left\{ \left| \sum_{m=1}^{M} c_m \chi_m - \tilde{I} \right|^2 + \alpha \sum_{m=1}^{M} |\nabla^{d+1} c_m|^2 |\chi_m|^2 \right.$$
$$\left. + \sum_{m=1}^{M} \left[\epsilon |\nabla \chi_m|^2 + \epsilon^{-1} |\chi_m (1 - \chi_m)|^2 \right] + \epsilon^{-1} \left| 1 - \sum_{m=1}^{M} \chi_m \right|^2 \right\}$$

Higher Order Segmentation

Forthcoming results with [Fürtinger]: Higher order Mumford Shah,

$$\min_{I,\Gamma} = \int_{\Omega} |I - \tilde{I}|^2 + \alpha \int_{\Omega \setminus \Gamma} |\nabla^{d+1} I|^2 + \beta |\Gamma|$$

Phase function (Ambrosio-Tortorelli) approximation:

$$\min_{I,\phi} = \int_{\Omega} \left\{ |I - \tilde{I}|^2 + \alpha |\nabla^{d+1} I|^2 \phi^2 + \epsilon |\nabla \phi|^2 + \epsilon^{-1} |1 - \phi|^2 \right\}$$

but ϕ is drawn to zero by varying strengths of discrete $|\nabla^{d+1} I|^2$.
Partition approximation: $I \to \sum_{m=1}^{M} c_m \chi_m$ ($M \leq 4$, 4CMT)

$$\min_{c_m, \chi_m} = \int_{\Omega} \left\{ \left| \sum_{m=1}^{M} c_m \chi_m - \tilde{I} \right|^2 + \alpha \sum_{m=1}^{M} |\nabla^{d+1} c_m|^2 |\chi_m|^2 \right.$$
$$\left. + \sum_{m=1}^{M} \left[\epsilon |\nabla \chi_m|^2 + \epsilon^{-1} |\chi_m (1 - \chi_m)|^2 \right] + \epsilon^{-1} \left| 1 - \sum_{m=1}^{M} \chi_m \right|^2 \right\}$$

Note: c_m determined on connected components of ($\chi_m = 1$).

Higher Order Registration

Forthcoming results with [Fürtinger]: Counterpart formulation,

$$\min_{c_0^m, \chi_0^m, c_1^m, \chi_1^m, \boldsymbol{u}} = \int_\Omega \left\{ \left| \sum_{m=1}^M c_0^m \chi_0^m - \tilde{I}_0 \right|^2 + \alpha \sum_{m=1}^M |\nabla^{d+1} c_0^m|^2 |\chi_0^m|^2 \right.$$

$$\left. + \sum_{m=1}^M \left[\epsilon |\nabla \chi_0^m|^2 + \epsilon^{-1} |\chi_0^m (1 - \chi_0^m)|^2 \right] + \epsilon^{-1} \left| 1 - \sum_{m=1}^M \chi_0^m \right|^2 \right.$$

Higher Order Registration

Forthcoming results with [Fürtinger]: Counterpart formulation,

$$\min_{c_0^m,\chi_0^m,c_1^m,\chi_1^m,\boldsymbol{u}} = \int_\Omega \left\{ \left| \sum_{m=1}^{M} c_0^m \chi_0^m - \tilde{I}_0 \right|^2 + \alpha \sum_{m=1}^{M} |\nabla^{d+1} c_0^m|^2 |\chi_0^m|^2 \right.$$

$$+ \left| \sum_{m=1}^{M} c_1^m \chi_1^m - \tilde{I}_1 \right|^2 + \alpha \sum_{m=1}^{M} |\nabla^{d+1} c_1^m|^2 |\chi_1^m|^2$$

$$+ \sum_{m=1}^{M} \left[\epsilon |\nabla \chi_0^m|^2 + \epsilon^{-1} |\chi_0^m (1 - \chi_0^m)|^2 \right] + \epsilon^{-1} \left| 1 - \sum_{m=1}^{M} \chi_0^m \right|^2$$

$$+ \sum_{m=1}^{M} \left[\epsilon |\nabla \chi_1^m|^2 + \epsilon^{-1} |\chi_1^m (1 - \chi_1^m)|^2 \right] + \epsilon^{-1} \left| 1 - \sum_{m=1}^{M} \chi_1^m \right|^2$$

Higher Order Registration

Forthcoming results with [Fürtinger]: Counterpart formulation,

$$
\begin{aligned}
\min_{c_0^m,\chi_0^m,c_1^m,\chi_1^m,\boldsymbol{u}} = \int_\Omega \Bigg\{ & \left|\sum_{m=1}^M c_0^m \chi_0^m - \tilde{I}_0\right|^2 + \alpha \sum_{m=1}^M |\nabla^{d+1} c_0^m|^2 |\chi_0^m|^2 \\
& + \left|\sum_{m=1}^M c_1^m \chi_1^m - \tilde{I}_1\right|^2 + \alpha \sum_{m=1}^M |\nabla^{d+1} c_1^m|^2 |\chi_1^m|^2 \\
& + \sum_{m=1}^M \left[\epsilon |\nabla \chi_0^m|^2 + \epsilon^{-1} |\chi_0^m (1-\chi_0^m)|^2\right] + \epsilon^{-1} \left|1 - \sum_{m=1}^M \chi_0^m\right|^2 \\
& + \sum_{m=1}^M \left[\epsilon |\nabla \chi_1^m|^2 + \epsilon^{-1} |\chi_1^m (1-\chi_1^m)|^2\right] + \epsilon^{-1} \left|1 - \sum_{m=1}^M \chi_1^m\right|^2 \\
& \sum_{m=1}^M |\chi_0^m \circ (\mathrm{Id} + \boldsymbol{u}) - \chi_1^m|^2 + \mu |\nabla \boldsymbol{u}^{\mathrm{T}} + \nabla \boldsymbol{u}|^2 \Bigg\}
\end{aligned}
$$

Ergodic Sequences

Temporal averages are (locally) equal to spatial averages:

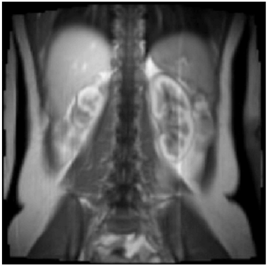

ave $t = 30 : 40$

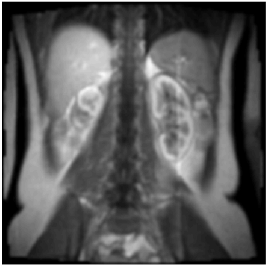

ave $x \in 5 \times 5$

Ergodic Sequences

Temporal averages are (locally) equal to spatial averages:

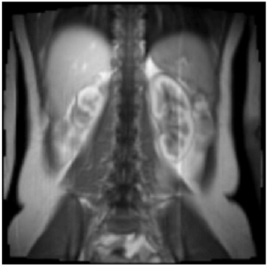

ave $t = 30 : 40$

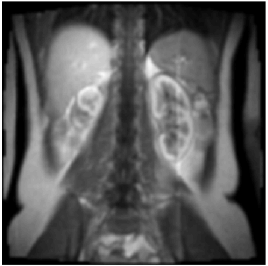

ave $x \in 5 \times 5$

Plan B: Given $\tilde{I} = \{\tilde{I}(\boldsymbol{x}, t)\}_{\boldsymbol{x}\in\Omega}^{t\in[0,T]}$ minimize

$$J(I, \boldsymbol{u}) = \int_0^T \int_\Omega \left\{ |\tilde{I} \circ (\mathrm{Id} + \boldsymbol{u}) - I|^2 + \alpha |I_t|^2 + \mu |\nabla \boldsymbol{u}^{\mathrm{T}} + \nabla \boldsymbol{u}|^2 \right\} d\boldsymbol{x} dt$$

to obtain $I = \{I(\boldsymbol{x}, t)\}_{\boldsymbol{x}\in\Omega}^{t\in[0,T]}$ manifesting less motion.

Ergodic Sequences

Temporal averages are (locally) equal to spatial averages:

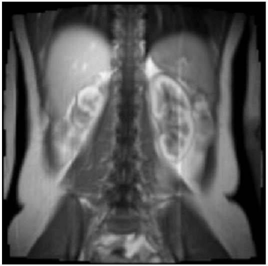

ave $t = 30 : 40$

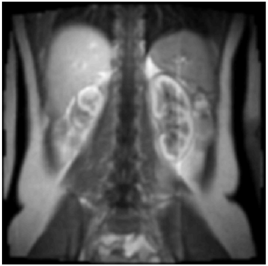

ave $x \in 5 \times 5$

Plan B: Given $\tilde{I} = \{\tilde{I}(\boldsymbol{x}, t)\}_{\boldsymbol{x}\in\Omega}^{t\in[0,T]}$ minimize

$$J(I, \boldsymbol{u}) = \int_0^T \int_\Omega \left\{ |\tilde{I} \circ (\mathrm{Id} + \boldsymbol{u}) - I|^2 + \alpha |I_t|^2 + \mu |\nabla \boldsymbol{u}^{\mathrm{T}} + \nabla \boldsymbol{u}|^2 \right\} d\boldsymbol{x} dt$$

to obtain $I = \{I(\boldsymbol{x}, t)\}_{\boldsymbol{x}\in\Omega}^{t\in[0,T]}$ manifesting less motion.

[Hofer, Keeling, Reishofer]

Registration of Whole Ergodic Sequences

Stepwise: Initialize $I_\mathrm{r} = \tilde{I} \circ (\mathrm{Id} + \boldsymbol{u})$ with $\boldsymbol{u} = 0$.
Then smooth temporally,

$$I_\mathrm{s}^{(\boldsymbol{x})} = \text{argmin} \int_0^T \left\{ |I_\mathrm{r} - I|^2 + \alpha |I_t|^2 \right\}^{(\boldsymbol{x})} dt$$

to obtain a registration target I_s.

Registration of Whole Ergodic Sequences

Stepwise: Initialize $I_{\mathrm{r}} = \tilde{I} \circ (\mathrm{Id} + \boldsymbol{u})$ with $\boldsymbol{u} = 0$.
Then smooth temporally,

$$I_{\mathrm{s}}^{(\boldsymbol{x})} = \operatorname{argmin} \int_0^T \left\{ |I_{\mathrm{r}} - I|^2 + \alpha |I_t|^2 \right\}^{(\boldsymbol{x})} dt$$

to obtain a registration target I_{s}.

- Original $\tilde{I}$ and target I_{s} have same intensity modulations.

Registration of Whole Ergodic Sequences

Stepwise: Initialize $I_{\mathrm{r}} = \tilde{I} \circ (\mathrm{Id} + \boldsymbol{u})$ with $\boldsymbol{u} = 0$.
Then smooth temporally,

$$I_{\mathrm{s}}^{(\boldsymbol{x})} = \operatorname{argmin} \int_0^T \left\{ |I_{\mathrm{r}} - I|^2 + \alpha |I_t|^2 \right\}^{(\boldsymbol{x})} dt$$

to obtain a registration target I_{s}.

- Original $\tilde{I}$ and target I_{s} have same intensity modulations.
- Target I_{s} is also spatially smoothed but manifests less motion.

Registration of Whole Ergodic Sequences

Stepwise: Initialize $I_\mathrm{r} = \tilde{I} \circ (\mathrm{Id} + \boldsymbol{u})$ with $\boldsymbol{u} = 0$.
Then smooth temporally,

$$I_\mathrm{s}^{(\boldsymbol{x})} = \mathrm{argmin} \int_0^T \left\{ |I_\mathrm{r} - I|^2 + \alpha |I_t|^2 \right\}^{(\boldsymbol{x})} dt$$

to obtain a registration target I_s.

- Original $\tilde{I}$ and target I_s have same intensity modulations.
- Target I_s is also spatially smoothed but manifests less motion.

Next: Register the two sequences,

$$\boldsymbol{u}^{(t)} = \mathrm{argmin} \int_\Omega \left\{ |\tilde{I} \circ (\mathrm{Id} + \boldsymbol{u}) - I_\mathrm{s}|^2 + \mu |\nabla \boldsymbol{u}^\mathrm{T} + \nabla \boldsymbol{u}|^2 \right\}^{(t)} d\boldsymbol{x}$$

and update $I_\mathrm{r} = \tilde{I} \circ (\mathrm{Id} + \boldsymbol{u})$.

Registration of Whole Ergodic Sequences

Stepwise: Initialize $I_{\mathrm{r}} = \tilde{I} \circ (\mathrm{Id} + \boldsymbol{u})$ with $\boldsymbol{u} = 0$.
Then smooth temporally,

$$I_{\mathrm{s}}^{(\boldsymbol{x})} = \operatorname{argmin} \int_0^T \left\{ |I_{\mathrm{r}} - I|^2 + \alpha |I_t|^2 \right\}^{(\boldsymbol{x})} dt$$

to obtain a registration target I_{s}.

- Original $\tilde{I}$ and target I_{s} have same intensity modulations.
- Target I_{s} is also spatially smoothed but manifests less motion.

Next: Register the two sequences,

$$\boldsymbol{u}^{(t)} = \operatorname{argmin} \int_\Omega \left\{ |\tilde{I} \circ (\mathrm{Id} + \boldsymbol{u}) - I_{\mathrm{s}}|^2 + \mu |\nabla \boldsymbol{u}^{\mathrm{T}} + \nabla \boldsymbol{u}|^2 \right\}^{(t)} d\boldsymbol{x}$$

and update $I_{\mathrm{r}} = \tilde{I} \circ (\mathrm{Id} + \boldsymbol{u})$.

Repeat: Until changes in I_{r} negligible.

Registration of Whole Ergodic Sequences

Stepwise: Initialize $I_{\mathrm{r}} = \tilde{I} \circ (\mathrm{Id} + \boldsymbol{u})$ with $\boldsymbol{u} = 0$.
Then smooth temporally,

$$I_{\mathrm{s}}^{(\boldsymbol{x})} = \operatorname{argmin} \int_0^T \left\{ |I_{\mathrm{r}} - I|^2 + \alpha |I_t|^2 \right\}^{(\boldsymbol{x})} dt$$

to obtain a registration target I_{s}.

- Original $\tilde{I}$ and target I_{s} have same intensity modulations.
- Target I_{s} is also spatially smoothed but manifests less motion.

Next: Register the two sequences,

$$\boldsymbol{u}^{(t)} = \operatorname{argmin} \int_\Omega \left\{ |\tilde{I} \circ (\mathrm{Id} + \boldsymbol{u}) - I_{\mathrm{s}}|^2 + \mu |\nabla \boldsymbol{u}^{\mathrm{T}} + \nabla \boldsymbol{u}|^2 \right\}^{(t)} d\boldsymbol{x}$$

and update $I_{\mathrm{r}} = \tilde{I} \circ (\mathrm{Id} + \boldsymbol{u})$.

Repeat: Until changes in I_{r} negligible. Result: [fixed point].

Thank you for your attention!

Registration of Edge Sets

For mapping a Purkinje fiber network system [Fürtinger]:

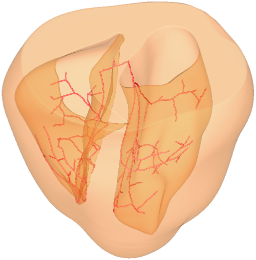

Registration of Edge Sets

For mapping a Purkinje fiber network system [Fürtinger]:

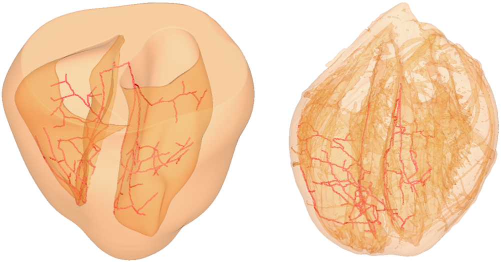

Performed using 2D slices,

$$\min_{u} \int_{\Omega} \left\{ |I_0^\epsilon \circ (\mathrm{Id} + u) - I_1^\epsilon|^2 + \mu |\nabla u^{\mathrm{T}} + \nabla u|^2 \right\}$$

Registration of Edge Sets

For mapping a Purkinje fiber network system [Fürtinger]:

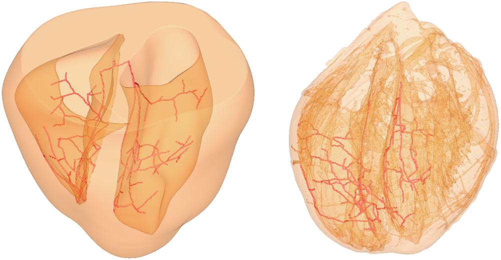

Performed using 2D slices,

$$\min_u \int_\Omega \left\{ |I_0^\epsilon \circ (\mathrm{Id} + u) - I_1^\epsilon|^2 + \mu |\nabla u^{\mathrm{T}} + \nabla u|^2 \right\}$$

with diffuse images:

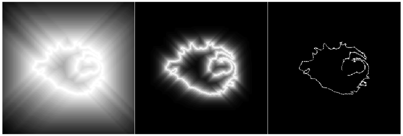

Registration of Edge Sets

For mapping a Purkinje fiber network system [Fürtinger]:

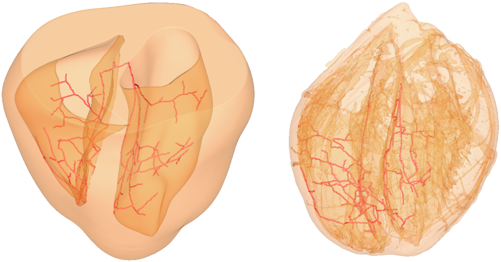

Performed using 2D slices,

$$\min_u \int_\Omega \left\{ |I_0^\epsilon \circ (\mathrm{Id} + u) - I_1^\epsilon|^2 + \mu |\nabla u^{\mathrm{T}} + \nabla u|^2 \right\}$$

with diffuse images:

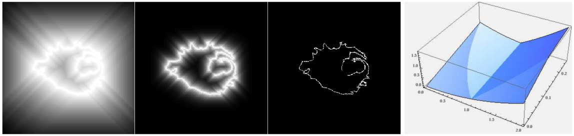

Reducing $\epsilon \to \epsilon_0 > 0$

$\epsilon_0 = 0 \Rightarrow \text{argmin} = 0!$